ELSEVIER

Engineering Analysis with Boundary Elements 30 (2006) 338–349

ENGINEERING ANALYSIS *with* BOUNDARY ELEMENTS

www.elsevier.com/locate/enganabound

Three-dimensional fundamental solutions for transient heat transfer by conduction in an unbounded medium, half-space, slab and layered media

António Tadeu *, Nuno Simões

Faculty of Sciences and Technology, Department of Civil Engineering, University of Coimbra, Pinhal de Marrocos, Polo II, 3030-290 Coimbra, Portugal

Received 11 August 2005; accepted 24 January 2006
Available online 5 April 2006

Abstract

This paper presents analytical Green's functions for the transient heat transfer phenomena by conduction, for an unbounded medium, half-space, slab and layered formation when subjected to a point heat source. The transient heat responses generated by a spherical heat source are computed as Bessel integrals, following the transformations proposed by Sommerfeld [Sommerfeld A. Mechanics of deformable bodies. New York: Academic Press; 1950; Ewing WM, Jardetzky WS, Press F. Elastic waves in layered media. New York: McGraw-Hill; 1957]. The integrals can be modelled as discrete summations, assuming a set of sources equally spaced along the vertical direction. The expressions presented here allow the heat field inside a layered formation to be computed without fully discretizing the interior domain or boundary interfaces.

The final Green's functions describe the conduction phenomenon throughout the domain, for a half-space and a slab. They can be expressed as the sum of the heat source and the surface terms. The surface terms need to satisfy the boundary conditions at the surfaces, which can be of two types: null normal fluxes or null temperatures. The Green's functions for a layered formation are obtained by adding the heat source terms and a set of surface terms, generated within each solid layer and at each interface. These surface terms are defined so as to guarantee the required boundary conditions, which are: continuity of temperatures and normal heat fluxes between layers.

This formulation is verified by comparing the frequency responses obtained from the proposed approach with those where a double-space Fourier transformation along the horizontal directions [Tadeu A, António J, Simões N. 2.5D Green's functions in the frequency domain for heat conduction problems in unbounded, half-space, slab and layered media. CMES: Computer Model Eng Sci 2004;6(1):43–58] is used. In addition, time domain solutions were compared with the analytical solutions that are known for the case of an unbounded medium, a half-space and a slab.

Keywords: Transient heat transfer; Conduction; 3D Green's functions; Layered media

1. Introduction

This work presents Green's functions for calculating the three-dimensional transient heat transfer by conduction in the presence of an unbounded, half-space, slab and multi-layer formations when heated by a point source. The problem is formulated in the frequency domain using time Fourier transforms. The proposed technique allows the use of any amplitude time evolution of the heat source. The proposed fundamental solutions relate the heat field variables (fluxes or temperatures) at some position in the domain caused by a heat source placed elsewhere in the media.

This work extends the previous work carried out by the authors to define the heat conduction response of layered solid media subjected to a spatially sinusoidal harmonic heat line source [3]. The technique described in that paper requires the knowledge of the Green's functions for the unbounded media. They are developed by first applying a time Fourier transform to the time diffusion equation for a heat point source and then a dual spatial Fourier transform to the resulting Helmholtz equation, along the two horizontal directions (x and z), in the frequency domain. So these functions are written first as a superposition of cylindrical heat waves along one horizontal direction (z) and then as a superposition of heat plane sources.

The Green's functions for a layered formation were formulated as the sum of the heat source terms equal to those in the full-space and the surface terms required to satisfy the boundary conditions at the interfaces, i.e. continuity of temperatures and normal heat fluxes between layers, and null normal fluxes or null temperatures at the outer surface. The total heat field was found by adding the heat source terms, equal to those in the unbounded space, to the sets of surface terms arising within each layer and at each interface.

* Corresponding author. Tel.: +351 239 797201; fax: +351 239 797190.
E-mail address: tadeu@dec.uc.pt (A. Tadeu).

0955-7997/$ - see front matter © 2006 Elsevier Ltd. All rights reserved.
doi:10.1016/j.enganabound.2006.01.011

In the work described here, the heat diffusion generated by a spherical heat source is computed as a Bessel integral, following the transformations proposed by Sommerfeld [1,2] in his study on the propagation of elastic waves. The resulting integrals are made discrete, assuming the existence of a set of sources equally spaced along the vertical direction.

In the presence of a layered formation, the heat diffusion within each layer is modelled using, at the two layer interfaces, surface terms that are similar to the source, with unknown amplitudes a priori. The amplitudes of these surface terms are defined by prescribing the existing boundary conditions at the solid interfaces (i.e. continuity of temperatures and normal heat fluxes between layers, and null normal fluxes or null temperatures at the outer surfaces).

These Green's functions are useful in themselves. However, they can also be incorporated into boundary element method (BEM) or method of fundamental solutions (MFS) algorithms to model the heat diffusion across layered media containing three-dimensional heterogeneities, without the discretization of the flat horizontal interfaces. The present Green's functions require much less computational effort than the earlier ones. However, it should be noted that the previously developed Green's functions, which require a dual spatial Fourier transform, are more suitable for solving layered media containing cylindrical heterogeneities.

This paper first presents the three-dimensional solution of a point heat diffusion source in an unbounded medium, explaining the mathematical manipulation required to obtain the solution as a Bessel integral in the frequency domain. The procedure to retrieve the time domain solutions is also given. This methodology is verified by comparing the results obtained with the exact time solutions.

This paper then goes on to describe the formulation for a point heat load applied to a half-space, a slab, a slab over a half-space medium and a layered formation. The continuity of temperature and heat fluxes need to be established between two neighbouring layers, while null temperatures or null heat fluxes may be prescribed along an external interface of the boundary. The full set of expressions is corroborated by comparing its frequency solutions with those provided by the previous formulation that requires a double spatial Fourier transform. Time solutions are verified in the case of a half-space and a slab, for which analytical solutions are known, by using an image model approach (see Carslaw and Jaeger [4]).

2. 3D problem formulation and Green's functions in an unbounded medium

The transient heat transfer by conduction in the x, y and z directions is expressed by the equation

$$\left(\frac{\partial^2}{\partial x^2}+\frac{\partial^2}{\partial y^2}+\frac{\partial^2}{\partial z^2}\right)T=\frac{1}{K}\frac{\partial T}{\partial t}, \tag{1}$$

in which t is time, $T(t,x,y,z)$ is temperature, $K=k/(\rho c)$ is the thermal diffusivity, k is the thermal conductivity, ρ is the density and c is the specific heat. The application of a Fourier transformation in the time domain to Eq. (1) gives the equation

$$\left(\left(\frac{\partial^2}{\partial x^2}+\frac{\partial^2}{\partial y^2}+\frac{\partial^2}{\partial z^2}\right)+\left(\sqrt{\frac{-\mathrm{i}\omega}{K}}\right)^2\right)\hat{T}(\omega,x,y,z)=0, \tag{2}$$

where $\mathrm{i}=\sqrt{-1}$ and ω is the frequency. For a heat point source, applied at (x_0,y_0,z_0) in an unbounded medium, of the form $p(\omega,x,y,z,t)=\delta(x-x_0)\delta(y-y_0)\delta(z-z_0)\mathrm{e}^{\mathrm{i}(\omega t)}$, where $\delta(x-x_0)$, $\delta(y-y_0)$ and $\delta(z-z_0)$ are Dirac-delta functions, the fundamental solution of Eq. (2) can be expressed as

$$\hat{T}_{\mathrm{f}}(\omega,x,y,z)=\frac{\mathrm{e}^{-\mathrm{i}\sqrt{-(\mathrm{i}\omega/K)}r_0}}{2kr_0} \tag{3}$$

with $r_0=\sqrt{(x-x_0)^2+(y-y_0)^2+(z-z_0)^2}$.

This solution can be expressed as a Bessel integral, following the transformations proposed by Sommerfeld [1,2]

$$\hat{T}_{\mathrm{f}}(\omega,x,y,z)=\frac{-\mathrm{i}}{2k}\int_0^\infty J_0(k_y r)\frac{k_y\,\mathrm{e}^{-\mathrm{i}\sqrt{-(\mathrm{i}\omega/K)-k_y^2}|y-y_0|}}{\sqrt{-\frac{\mathrm{i}\omega}{K}-k_y^2}}\mathrm{d}k_y, \tag{4}$$

where $J_0(\,)$ are Bessel functions of order 0, k_y is the vertical wavenumber along the y direction and $r=\sqrt{(x-x_0)^2+(z-z_0)^2}$.

This integral can be expressed as a discrete sum if we assume the existence of virtual sources, equally spaced at L_y, along the vertical direction y,

$$\hat{T}_{\mathrm{f}}(\omega,x,y,z)=\frac{-\mathrm{i}\pi}{L_y k}\sum_{n=1}^{N}J_0(k_n r)\frac{k_n}{\nu_n}\mathrm{e}^{-\mathrm{i}\nu_n|y-y_0|} \tag{5}$$

with $\nu_n=\sqrt{-(\mathrm{i}\omega/K)-k_n^2}$, $k_n=(2\pi/L_y)n$. The distance L_y is chosen so as to prevent spatial contamination from the virtual sources, i.e. it must not be too small [5].

2.1. Responses in the time domain

The heat in the spatial–temporal domain is calculated by applying a numerical inverse fast Fourier transform in the frequency domain. The computations are performed using complex frequencies with a small imaginary part of the form $\omega_{\mathrm{c}}=\omega-\mathrm{i}\eta$ (with $\eta=0.7\,\Delta\omega$, and $\Delta\omega$ being the frequency step) to prevent interference from aliasing phenomena. In the time domain, this effect is removed by rescaling the response with an exponential window of the form $\mathrm{e}^{\eta t}$ [6]. The time variation of the source can be arbitrary. The time Fourier transformation of the source heat field defines the frequency domain to be computed. The response may need to be computed from 0.0 Hz up to very high frequencies. However, as the heat responses decay very rapidly as the frequency increases, we may set an upper limit on the frequency for which the solution is required.

2.2. Verification of the solution

The formulation described above was implemented and used to compute the heat field in an unbounded medium. In order to verify this formulation, the solution is verified in both the frequency and time domains. In the frequency domain, this verification is performed against solutions obtained using

a double-space Fourier transformation along the horizontal directions (2.5D formulation). In the case of the time domain solutions, the responses are compared with those provided by analytical responses. When the heat source is applied at point (X_0, Y_0, Z_0) at time $t=t_0$, the exact temperature evolution at (x,y,z) is given by the expression

$$T(t,x,y,z) = \frac{e^{-((x-x_0)^2+(y-y_0)^2+(z-z_0)^2)/4K\tau}}{\rho c(4\pi K\tau)^{3/2}}, \quad \text{if } t > t_0, \tag{6}$$

where $\tau = t - t_0$ (see Carslaw and Jaeger [4] and Banerjee [7]).

In the verification procedure, a homogeneous unbounded medium, with thermal properties that took $k=1.4$ W m^{-1} °C^{-1}, $c=880$ J kg^{-1} °C^{-1} and $\rho=2300$ kg m^{-3}, was excited at $t=0.0$ s by a unit heat source placed at $x=0.0$ m, $y=1.0$ m.

The heat responses generated by a spherical unit heat source were calculated for three different receivers: Rec. 1, Rec. 2 and Rec. 3, placed, respectively, at (0.2,0.5,0.0) m, (0.2,0.5,0.5) m and (0.2,0.5,1.0) m.

The calculations in this case, and in all examples presented below for other cases, were first performed in the frequency range $[0.0, 1024.0\times10^{-7}]$ Hz with an increment of $\Delta\omega = 1\times10^{-7}$ Hz, which defines a time window of $T=$ 2777.8 h. Complex frequencies of the form $\omega_c = \omega - i0.7\Delta\omega$ have been used to avoid the aliasing phenomenon. The spatial period has been set as $L_y = 2\sqrt{k_y/(\rho c\Delta f)}$. Fig. 1(a)–(c) displays the responses in the frequency domain at the receivers Rec. 1, 2 and 3 for the first 320 frequencies: the solid lines identify the responses using the proposed Green's functions, while the marks show the response obtained using a double-space Fourier transformation along the horizontal directions (2.5D Green's functions formulation). Fig. 1(d) illustrates the good agreement between the exact time solution calculated given by Eq. (6), represented by solid lines, and the response obtained using the proposed Green's functions, symbolized by marks, for the same three receivers. The mean errors shown in Fig. 1(d) obtained from the average of the difference between the proposed solutions and the analytical time domain solutions for these three receivers are, respectively, 6.66×10^{-12}, 6.46×10^{-12} and 6.30×10^{-12} °C.

3. Green's functions in a half-space

In this section, a semi-infinite medium bounded by a surface with null heat fluxes or null temperatures is considered. The required Green's functions of the proposed formulation for a half-space can be expressed as the sum of the surface terms and the source terms. The surface terms need to satisfy the boundary condition of the surface (null heat fluxes or null temperatures), while the source terms are equal to those presented for the infinite unbounded medium. The surface terms for a heat source located at (x_0,y_0,z_0) can be expressed by

$$\hat{T}_1(\omega,x,y,z) = \frac{-i\pi}{L_y k}\sum_{n=1}^{N} A_n \frac{k_n}{\nu_n} J_0(k_n r) e^{-i\nu_n|y|}. \tag{7}$$

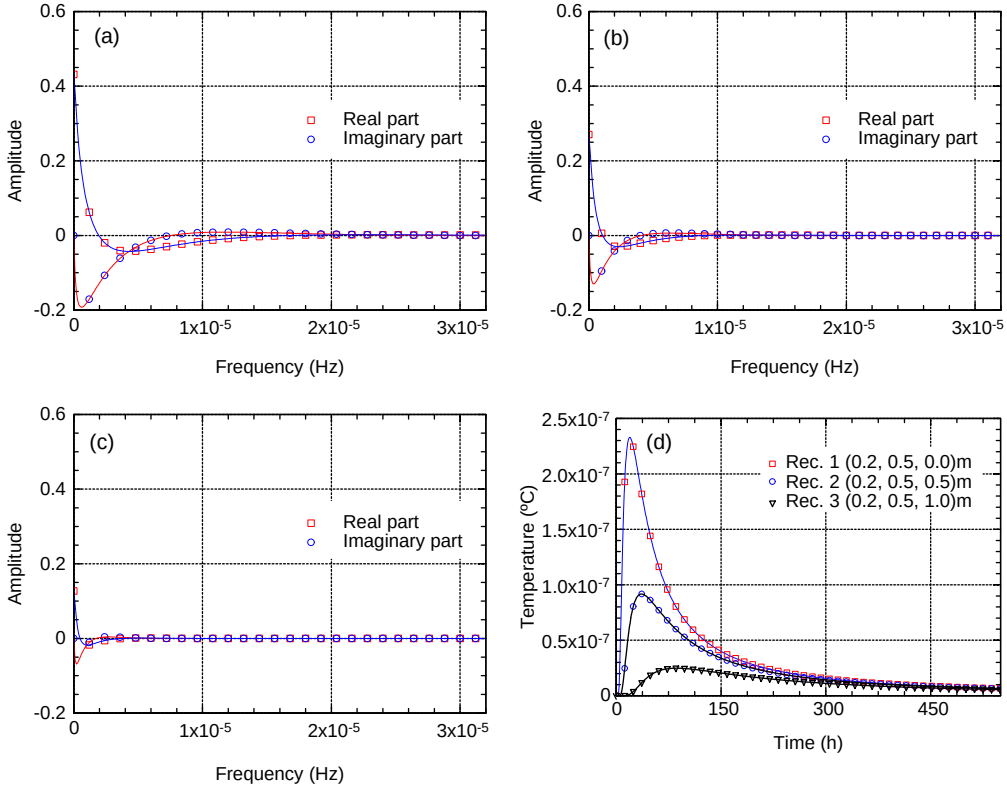

Fig. 1. Unbounded medium: frequency responses at receivers Rec. 1 (a), Rec. 2 (b) and Rec. 3 (c) for a spherical unit heat source applied at point (0.0,1.0,0.0) m. (d) Temperature curves at receivers Rec. 1, Rec. 2 and Rec. 3.

A_n is the unknown coefficient to be computed, so that the heat field produced simultaneously by the source

$$\left(\hat{T}_{\text{inc}}(\omega,x,y,z)=\frac{-\mathrm{i}\pi}{L_y k}\sum_{n=1}^{N}J_0(k_n r)\frac{k_n}{\nu_n}\mathrm{e}^{-\mathrm{i}\nu_n|y-y_0|}\right),$$

and surface terms should produce $\hat{T}_1(\omega,x,y,z)=0$ or $\partial\hat{T}_1(\omega,x,y,z)/\partial y=0$ at $y=0$.

The computation of the unknown coefficient is obtained for each value of n. These coefficients are given below for the two cases of null heat fluxes and null temperatures at the surface $y=0$.

Null normal flux at $y=0$

$$A_n=\mathrm{e}^{-\mathrm{i}\nu_n y_0}.$$

Null temperature at $y=0$

$$A_n=-\mathrm{e}^{-\mathrm{i}\nu_n y_0}. \tag{8}$$

Replacing these coefficients in Eq. (7), we may compute the heat terms associated with the surface.

Null normal flux at $y=0$

$$\hat{T}_1(\omega,x,y,z)=\frac{-\mathrm{i}\pi}{L_y k}\sum_{n=1}^{N}\frac{k_n}{\nu_n}J_0(k_n r)\mathrm{e}^{-\mathrm{i}\nu_n|y+y_0|}.$$

Null temperature at $y=0$

$$\hat{T}_1(\omega,x,y,z)=\frac{\mathrm{i}\pi}{L_y k}\sum_{n=1}^{N}\frac{k_n}{\nu_n}J_0(k_n r)\mathrm{e}^{-\mathrm{i}\nu_n|y+y_0|}. \tag{9}$$

The final fundamental solutions for a half-space are given by adding these terms, the source and the surface terms, which leads to:

Null normal flux at $y=0$

$$\hat{T}(\omega,x,y,z)=\frac{-\mathrm{i}\pi}{L_y k}\sum_{n=1}^{N}\frac{k_n}{\nu_n}J_0(k_n r)(\mathrm{e}^{-\mathrm{i}\nu_n|y|}+\mathrm{e}^{-\mathrm{i}\nu_n|y+y_0|}). \tag{10}$$

Null temperature at $y=0$

$$\hat{T}(\omega,x,y,z)=\frac{-\mathrm{i}\pi}{L_y k}\sum_{n=1}^{N}\frac{k_n}{\nu_n}J_0(k_n r)(\mathrm{e}^{-\mathrm{i}\nu_n|y|}-\mathrm{e}^{-\mathrm{i}\nu_n|y+y_0|}). \tag{11}$$

The final heat field in the time domain is calculated by applying a numerical inverse fast Fourier transform in the frequency domain.

The time domain solution can also be obtained using the image model technique. In this approach, the solution can be achieved by superposing the heat field generated by virtual sources with positive or negative polarity in such a way as to simulate null temperatures or null heat fluxes at the surface.

Null normal flux at $y=0$

$$T(t,x,y,z)=\frac{\mathrm{e}^{(-r_0/4K\tau)}+\mathrm{e}^{(-r_1/4K\tau)}}{\rho c(4\pi K\tau)^{3/2}}.$$

Null temperature at $y=0$

$$T(t,x,y,z)=\frac{\mathrm{e}^{(-r_0/4K\tau)}-\mathrm{e}^{(-r_1/4K\tau)}}{\rho c(4\pi K\tau)^{3/2}} \tag{12}$$

in which $\tau=t-t_0$, $r_0=(x-x_0)^2+(y-y_0)^2+(z-z_0)^2$ and $r_1=(x-x_0)^2+(y+y_0)^2+(z-z_0)^2$.

3.1. Verification of the solution

The solutions derived before [3], using a double space Fourier transformation along the horizontal directions (2.5D formulation), which entails higher computational costs, are used to verify the response in the frequency domain. The time domain solutions are also evaluated using the image model technique.

The verification of the solution is illustrated for a homogeneous half-space medium with thermal material properties that take $k=1.4$ W m^{-1} °C^{-1}, $c=880.0$ J kg^{-1} °C^{-1} and $\rho=230$ kg m^{-3}. This structure is excited at (0.0,1.0,0.0) m by a point heat source. Fig. 2 gives the total amplitudes (source and surface terms summation) in the frequency domain obtained at the receivers Rec. 1 and Rec. 2, placed at (0.2,0.5,0.0) m and (0.2,0.5,0.5) m, for both null normal flux and null temperatures at $y=0$, in the frequency range [0.0, 320.0×10^{-7}] Hz. In this plot, the real and imaginary parts of the response are given: solid lines represent the results provided by the proposed solutions, while the marks correspond to the 2.5D formulation solutions. These results show that the responses are similar.

In addition, the results in the time domain provided by the proposed formulation are compared with those obtained directly in the time domain using the image model technique, at three different receivers (see Fig. 3). This figure shows similar results for the image model technique solutions, which are plotted with solid lines, and the proposed formulation results, represented by marks. The mean errors of the results shown in Fig. 3, obtained from the average of the difference between the proposed solutions and the analytical time domain solutions for these three receivers, are listed in Table 1.

4. Green's functions in a slab formation

For a slab structure with thickness h, the Green's functions can be found taking into account the null heat fluxes or null temperatures prescribed at each surface. They can be expressed by adding the surface and source terms, which are equal to those in the full-space.

Three scenarios can be considered: null heat fluxes at the top and bottom interfaces (*Case I*); null temperatures in both surface boundaries (*Case II*), and different conditions at each surface (*Case III*). At the top and bottom interfaces, surface terms can be generated and expressed in a form similar to that of the source term.

Top surface medium

$$\hat{T}_1(\omega,x,y,z)=\frac{-\mathrm{i}\pi}{L_y k}\sum_{n=1}^{N}A_n^t\frac{k_n}{\nu_n}J_0(k_n r)\mathrm{e}^{-\mathrm{i}\nu_n|y|}.$$

Bottom surface medium

$$\hat{T}_2(\omega,x,y,z)=\frac{-\mathrm{i}\pi}{L_y k}\sum_{n=1}^{N}A_n^b\frac{k_n}{\nu_n}J_0(k_n r)\mathrm{e}^{-\mathrm{i}\nu_n|y-h|}. \tag{13}$$

A_n^t and A_n^b are as yet unknown coefficients to be determined by imposing the appropriate boundary conditions, so that the field originated simultaneously by the source and the surface

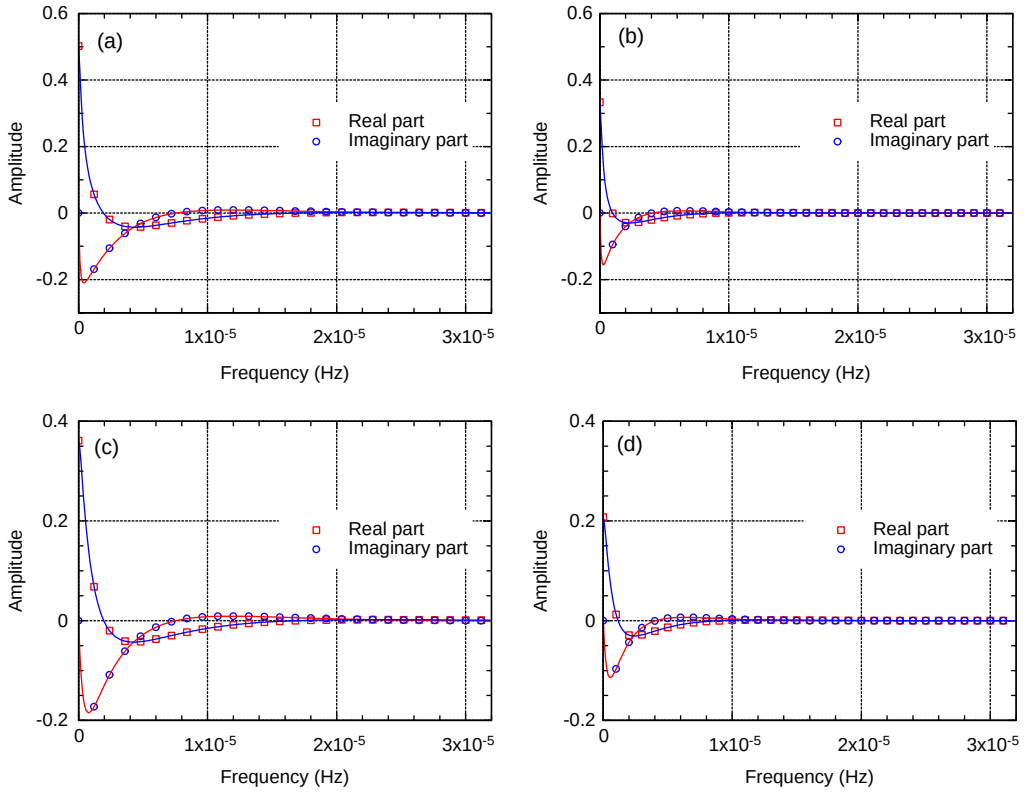

Fig. 2. Real and imaginary parts of the response for a half-space formation, when a heat source is applied at point (0.0,1.0,0.0) m: (a) Receiver 1 for null normal flux at $y=0$; (b) Receiver 2 for null normal flux at $y=0$; (c) Receiver 1 for null temperature at $y=0$; (d) Receiver 2 for null temperature at $y=0$.

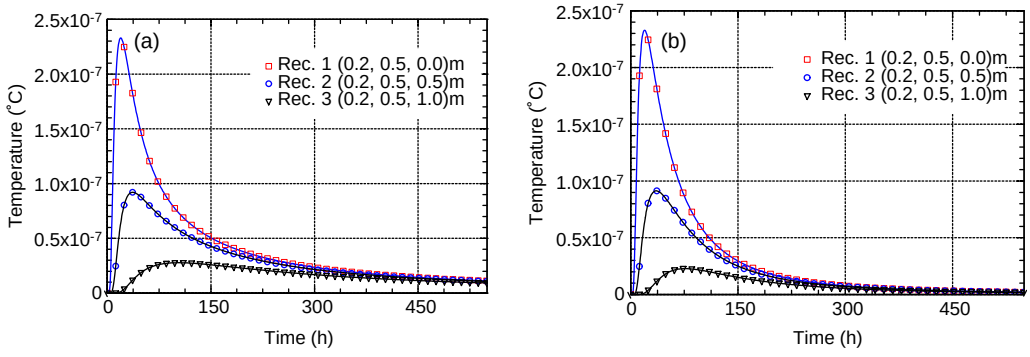

Fig. 3. Temperature curves for a half-space formation at receivers Rec. 1, Rec. 2 and Rec. 3, when a heat source is applied at point (0.0,1.0,0.0) m: (a) null normal flux at $y=0$; (b) null temperature at $y=0$.

terms guarantees null heat fluxes or null temperatures at $y=0$ and h.

This problem formulation leads to a system of two equations in the two unknown constants for each value of n.

Case I: null heat fluxes at the top and bottom surfaces

$$\begin{bmatrix} -\mathrm{i}\nu_n & \mathrm{i}\nu_n\, \mathrm{e}^{-\mathrm{i}\nu_n h} \\ -\mathrm{i}\nu_n\, \mathrm{e}^{-\mathrm{i}\nu_n h} & \mathrm{i}\nu_n \end{bmatrix} \begin{bmatrix} A_n^t \\ A_n^b \end{bmatrix} = \begin{bmatrix} -\mathrm{i}\nu_n\, \mathrm{e}^{-\mathrm{i}\nu_n y_0} \\ \mathrm{i}\nu_n\, \mathrm{e}^{-\mathrm{i}\nu_n |h-y_0|} \end{bmatrix}. \tag{14}$$

Case II: null temperatures at the top and bottom surfaces

$$\begin{bmatrix} 1 & \mathrm{e}^{-\mathrm{i}\nu_n h} \\ \mathrm{e}^{-\mathrm{i}\nu_n h} & 1 \end{bmatrix} \begin{bmatrix} A_n^t \\ A_n^b \end{bmatrix} = \begin{bmatrix} -\mathrm{e}^{-\mathrm{i}\nu_n y_0} \\ -\mathrm{e}^{-\mathrm{i}\nu_n |h-y_0|} \end{bmatrix}. \tag{15}$$

Case III: null heat fluxes at the top surface and null temperatures at the bottom surface

$$\begin{bmatrix} -\mathrm{i}\nu_n & \mathrm{i}\nu_n\, \mathrm{e}^{-\mathrm{i}\nu_n h} \\ \mathrm{e}^{-\mathrm{i}\nu_n h} & 1 \end{bmatrix} \begin{bmatrix} A_n^t \\ A_n^b \end{bmatrix} = \begin{bmatrix} -\mathrm{i}\nu_n\, \mathrm{e}^{-\mathrm{i}\nu_n y_0} \\ -\mathrm{e}^{-\mathrm{i}\nu_n |h-y_0|} \end{bmatrix}. \tag{16}$$

Once this system of equations has been solved, the amplitude of the surface terms has been fully defined, and

Table 1
Time domain mean errors for a half-space formation

	Null normal flux at $y=0$	Null temperature at $y=0$
Rec. 1	1.27×10^{-11} °C	8.89×10^{-13} °C
Rec. 2	1.22×10^{-11} °C	4.15×10^{-13} °C
Rec. 3	1.25×10^{-11} °C	4.03×10^{-13} °C

the heat in the slab can thus be found. The final expressions for the Green's functions are then derived from the sum of the source terms and the surface terms originated in the two slab surfaces, which leads to the following expressions

$$\hat{T}(\omega,x,y,z)=\frac{e^{-i\sqrt{(-(i\omega/K))}r_0}}{2kr_0}+\frac{-i\pi}{L_y k}\sum_{n=1}^{N}J_0(k_n r)\frac{k_n}{\nu_n}\times(A_n^t\,e^{-i\nu_n|y|}+A_n^b\,e^{-i\nu_n|y-h|}). \tag{17}$$

Once again, the heat field in the time domain can be calculated from a numerical inverse fast Fourier transform applied in the frequency domain.

In addition, the time solution can be achieved by superposing the heat field generated by virtual sources with positive or negative polarity (image model technique), and located to ensure the desired boundary conditions. For a slab, the image model technique needs a set of virtual sources to be placed in such a way as to simulate null temperatures or null heat fluxes at the surfaces.

Case I: null heat fluxes at the top and bottom surfaces

$$T(t,x,y,z)=\frac{e^{-r_0/4K\tau}}{\rho c(4\pi K\tau)^{3/2}}+\sum_{n=1}^{NS}\frac{e^{-r_1/4K\tau}+e^{-r_2/4K\tau}+e^{-r_3/4K\tau}+e^{-r_4/4K\tau}}{\rho c(4\pi K\tau)^{3/2}}. \tag{18}$$

Case II: null temperatures at the top and bottom surfaces

$$T(t,x,y,z)=\frac{e^{-r_0/4K\tau}}{\rho c(4\pi K\tau)^{3/2}}+\sum_{n=1}^{NS}\frac{-e^{-r_1/4K\tau}-e^{-r_2/4K\tau}+e^{-r_3/4K\tau}+e^{-r_4/4K\tau}}{\rho c(4\pi K\tau)^{3/2}}. \tag{19}$$

Case III: null heat fluxes at the top surface and null temperatures at the bottom surface

$$T(t,x,y,z)=\frac{e^{-r_0/4K\tau}}{\rho c(4\pi K\tau)^{3/2}}+\sum_{n=1}^{NS}(-1)^{n-1}\frac{e^{-r_1/4K\tau}-e^{-r_2/4K\tau}-e^{-r_3/4K\tau}-e^{-r_4/4K\tau}}{\rho c(4\pi K\tau)^{3/2}} \tag{20}$$

in which $\tau=t-t_0$, $r_0=(x-x_0)^2+(y-y_0)^2+(z-z_0)^2$, $r_1=(x-x_0)^2+(y+y_0+2h(n-1))^2+(z-z_0)^2$, $r_2=(x-x_0)^2+(y+y_0-2hn)^2+(z-z_0)^2$, $r_3=(x-x_0)^2+(y-y_0+2hn)^2+(z-z_0)^2$ and $r_4=(x-x_0)^2+(y-y_0-2hn)^2+(z-z_0)^2$.

4.1. Verification of the solution

The formulation described above for the slab formation was used to compute the responses at a receiver placed in a slab 2.0 m thick. The frequency domain results for the three boundary situations assumed were then compared with those given by a 2.5D formulation [3] for two different receivers: Rec. 1, placed at (0.2,0.5,0.0) m, and Rec. 2, localised at (0.2,0.5,0.5) m. An additional verification is performed in the time domain against the solutions provided by the image model technique described above. In this verification procedure, the medium properties remain the same as those assumed for the half-space ($k=1.4$ W m^{-1} °C^{-1}, $c=880.0$ J kg^{-1} °C^{-1} and $\rho=2300.0$ kg m^{-3}). The slab is heated by a harmonic point heat source applied at (0.0,1.0,0.0) m.

Fig. 4 shows the real and imaginary parts of the total responses, given by the sum of the source and surface terms, at the receivers Rec. 1 and Rec. 2 for the three different cases described above. The solid lines represent the proposed frequency responses, while the marked points correspond to the 2.5D formulation solution [3]. The results confirm that the solutions to the three cases are in very close agreement.

Fig. 5 provides the time domain solutions calculated by the proposed formulation and identified with marks. These are in good agreement with the results obtained with the image model technique and are plotted using solid lines. The calculations were obtained at three different receivers for the three cases with their different surface conditions. The mean errors of the results shown in Fig. 5, obtained from the average of the difference between the proposed solutions and the analytical time domain solutions for these three receivers, are listed in Table 2.

5. Green's functions in a layered formation

The solutions for more complex structures, such as a layer over a half-space, a layer bounded by two semi-infinite media and a multi-layer can be established imposing the required boundary conditions at the interfaces and at the free surface.

5.1. Layer over a half-space

Assuming the presence of a layer, h_1 thick, over a half-space, we may prescribe null temperature or null heat fluxes at the free surface (top), while at the interface we need to satisfy the continuity of temperature and normal heat fluxes. The solution is again expressed as the sum of the source terms (the incident field) equal to those in the full-space and the surface terms. At the interfaces 1 and 2, surface terms are generated, which can be expressed in a form analogous to that of the source term.

Layer interface 1

$$\hat{T}_{11}(\omega,x,y,z)=\frac{-i\pi}{L_y k_1}\sum_{n=1}^{N}A_{n1}^t\frac{k_n}{\nu_{n1}}J_0(k_n r)e^{-i\nu_{n1}|y|}. \tag{21}$$

Layer interface 2

$$\hat{T}_{12}(\omega,x,y,z)=\frac{-i\pi}{L_y k_1}\sum_{n=1}^{N}A_{n1}^b\frac{k_n}{\nu_{n1}}J_0(k_n r)e^{-i\nu_{n1}|y-h_1|}. \tag{22}$$

Half-space (interface 2)

$$\hat{T}_{21}(\omega,x,y,z)=\frac{-i\pi}{L_y k_2}\sum_{n=1}^{N}A_{n2}^t\frac{k_n}{\nu_{n2}}J_0(k_n r)e^{-i\nu_{n2}|y-h_1|}, \tag{23}$$

where $\nu_{nj}=\sqrt{-(i\omega/K_j)-k_n^2}$ with $\mathrm{Im}(\nu_{nj})\leq 0$ and h_1 is the layer thickness ($j=1$ stands for the layer (medium 1), while $j=2$

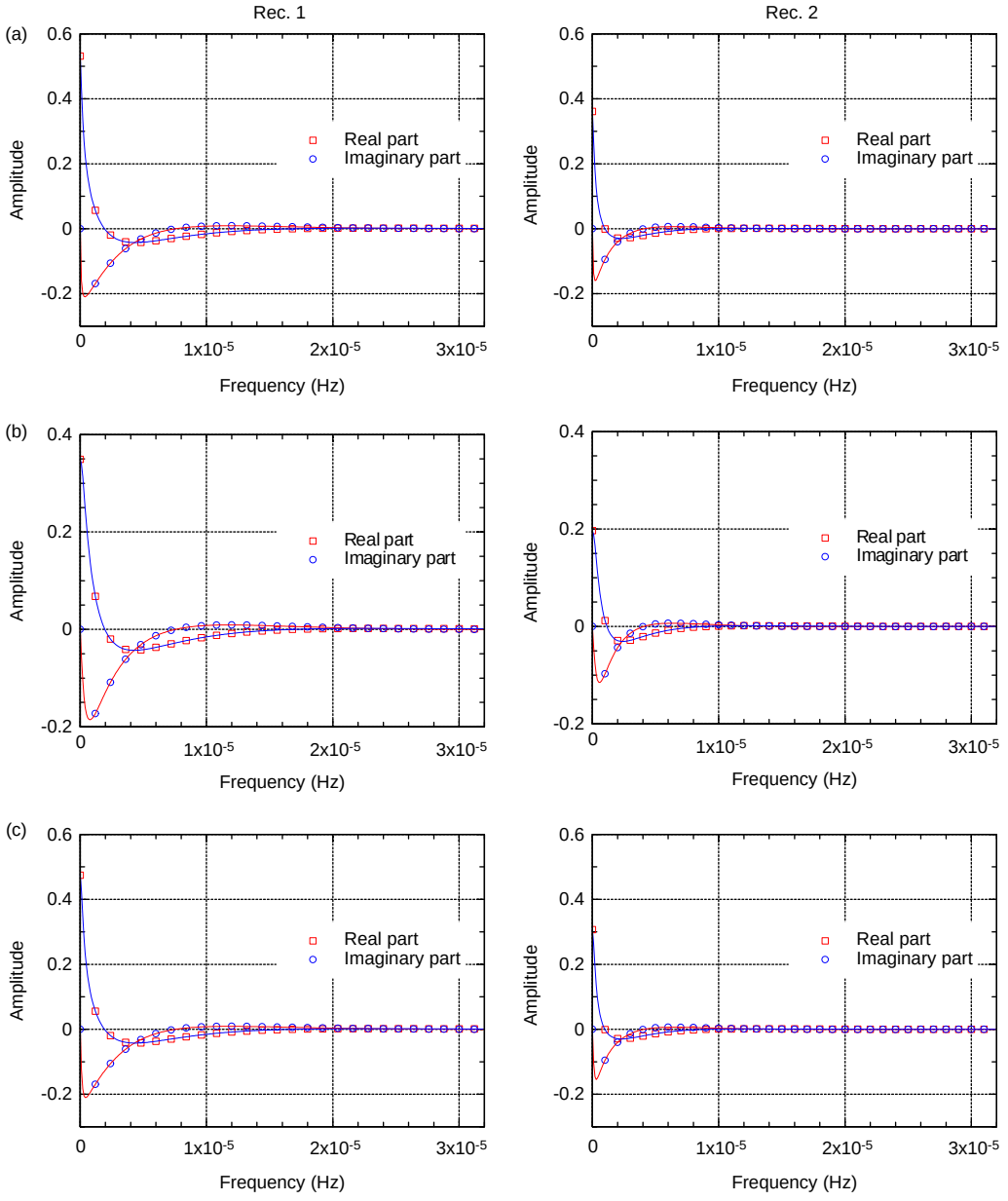

Fig. 4. Real and imaginary parts of the responses for a slab formation at receivers Rec. 1 and Rec.2, when a heat source is applied at point (0.0,1.0,0.0) m: (a) *Case I* (null heat flux at the top and bottom surfaces); (b) *Case II* (null temperature at the top and bottom surfaces); and (c) *Case III* (null temperature at the top surface and null heat flux at the bottom surface).

indicates the half-space (medium 2)). Meanwhile, $K_j=(k_j/\rho_j c_j)$ is the thermal diffusivity in the medium j (k_j, ρ_j and c_j are the thermal conductivity, the density and the specific heat of the material in the medium j, respectively).

The coefficients A^t_{n1}, A^b_{n1} and A^t_{n2} are as yet unknown. They are defined in order to ensure the appropriate boundary conditions: the field produced simultaneously by the source and surface terms allows the continuity of heat fluxes and temperatures at $y=h_1$, and null heat fluxes (*Case I*) or null temperatures (*Case II*) at $y=0$.

Imposing the three stated boundary conditions for each value of n, a system of three equations in the three unknown coefficients is defined.

Case I: null heat fluxes at $y=0$.

$$\begin{bmatrix} -\mathrm{i}\nu_{n1} & \mathrm{i}\nu_{n1}\,\mathrm{e}^{-\mathrm{i}\nu_{n1}h_1} & 0 \\ -\mathrm{i}\nu_{n1}\,\mathrm{e}^{-\mathrm{i}\nu_{n1}h_1} & \mathrm{i}\nu_{n1} & \mathrm{i}\nu_{n1} \\ \mathrm{e}^{-\mathrm{i}\nu_{n1}h_1} & 1 & -\dfrac{k_1\nu_{n1}}{k_2\nu_{n2}} \end{bmatrix} \begin{bmatrix} A^t_{n1} \\ A^b_{n1} \\ A^t_{n2} \end{bmatrix} = \begin{bmatrix} b_1 \\ b_2 \\ b_3 \end{bmatrix}, \tag{24}$$

where

$b_1=-\nu_{n1}\,\mathrm{e}^{-\mathrm{i}\nu_{n1}y_0}$,
$b_2=\mathrm{i}\nu_{n1}\,\mathrm{e}^{-\mathrm{i}\nu_{n1}|h_1-y_0|}$,
$b_3=-\mathrm{e}^{-\mathrm{i}\nu_{n1}|h_1-y_0|}$, when the source is in the layer ($y_0<h_1$),

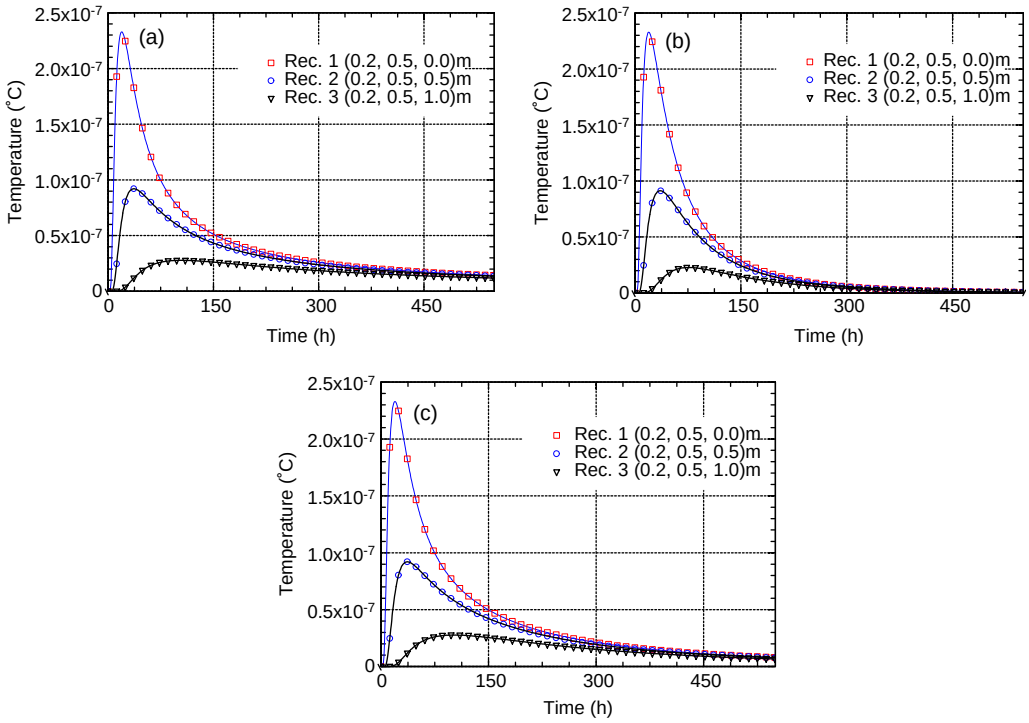

Fig. 5. Temperature curves for a slab formation at receivers Rec. 1 and Rec.2, when a heat source is applied at the point (0.0,1.0,0.0) m: (a) *Case I* (null heat flux at the top and bottom surfaces); (b) *Case II* (null temperature at the top and bottom surfaces); and (c) *Case III* (null temperature at the top surface and null heat flux at the bottom surface).

while

$b_1 = 0$,
$b_2 = \mathrm{i}\nu_{n1}\, \mathrm{e}^{-\mathrm{i}\nu_{n2}|h_1 - y_0|}$,
$b_3 = (k_1\nu_{n1}/k_2\nu_{n2})\mathrm{e}^{-\mathrm{i}\nu_{n2}|h_1 - y_0|}$, when the source is in the half-space ($y_0 > h_1$).

Case II: null temperatures at $y = 0$.

$$\begin{bmatrix} 1 & \mathrm{e}^{-\mathrm{i}\nu_{n1}h_1} & 0 \\ -\mathrm{i}\nu_{n1}\,\mathrm{e}^{-\mathrm{i}\nu_{n1}h_1} & \mathrm{i}\nu_{n1} & \mathrm{i}\nu_{n1} \\ \mathrm{e}^{-\mathrm{i}\nu_{n1}h_1} & 1 & -\dfrac{k_1\nu_{n1}}{k_2\nu_{n2}} \end{bmatrix} \begin{bmatrix} A^t_{n1} \\ A^b_{n1} \\ A^t_{n2} \end{bmatrix} = \begin{bmatrix} b_1 \\ b_2 \\ b_3 \end{bmatrix}, \qquad (25)$$

where

$b_1 = -\mathrm{e}^{-\mathrm{i}\nu_{n1}y_0}$,
$b_2 = \mathrm{i}\nu_{n1}\, \mathrm{e}^{-\mathrm{i}\nu_{n1}|h_1 - y_0|}$,
$b_3 = -\mathrm{e}^{-\mathrm{i}\nu_{n1}|h_1 - y_0|}$, when the source is in the layer ($y_0 < h_1$),

while

$b_1 = 0$,
$b_2 = \mathrm{i}\nu_{n1}\, \mathrm{e}^{-\mathrm{i}\nu_{n2}|h_1 - y_0|}$,
$b_3 = (k_1\nu_{n1}/k_2\nu_{n2})\mathrm{e}^{-\mathrm{i}\nu_{n2}|h_1 - y_0|}$, when the source is in the half-space ($y_0 > h_1$).

The heat field produced within the two media results from the contribution of both the surface terms generated at the various interfaces and the source term.

$y_0 < h_1$ (*source in the medium 1*)

$$\hat{T}(\omega,x,y,z) = \frac{\mathrm{e}^{-\mathrm{i}\sqrt{-(\mathrm{i}\omega/K_1)}r_0}}{2k_1 r_0} + \frac{-\mathrm{i}\pi}{L_y k_1}\sum_{n=1}^{N} J_0(k_n r)\frac{k_n}{\nu_{n1}} \times (A^t_{n1}\,\mathrm{e}^{-\mathrm{i}\nu_{n1}|y|} + A^b_{n1}\,\mathrm{e}^{-\mathrm{i}\nu_{n1}|y-h|}), \quad \text{if } y < h_1;$$

$$\hat{T}(\omega,x,y,z) = \frac{-\mathrm{i}\pi}{L_y k_2}\sum_{n=1}^{N} A^t_{n2}\frac{k_n}{\nu_{n2}} J_0(k_n r)\mathrm{e}^{-\mathrm{i}\nu_{n2}|y-h_1|}, \quad \text{if } y > h_1, \qquad (26)$$

$y_0 > h_1$ (*source in the medium 2*)

$$\hat{T}(\omega,x,y,z) = \frac{-\mathrm{i}\pi}{L_y k_1}\sum_{n=1}^{N} J_0(k_n r)\frac{k_n}{\nu_{n1}}(A^t_{n1}\,\mathrm{e}^{-\mathrm{i}\nu_{n1}|y|} + A^b_{n1}\,\mathrm{e}^{-\mathrm{i}\nu_{n1}|y-h|}), \quad \text{if } y < h_1;$$

$$\hat{T}(\omega,x,y,z) = \frac{\mathrm{e}^{-\mathrm{i}\sqrt{-(\mathrm{i}\omega/K_2)}r_0}}{2k_2 r_0} + \frac{-\mathrm{i}\pi}{L_y k_2} \times \sum_{n=1}^{N} A^t_{n2}\frac{k_n}{\nu_{n2}} J_0(k_n r)\mathrm{e}^{-\mathrm{i}\nu_{n2}|y-h_1|}, \quad \text{if } y > h_1. \qquad (27)$$

Table 2
Time domain mean errors for a slab formation

	Case I	Case II	Case III
Rec. 1	3.16×10^{-11} °C	1.00×10^{-12} °C	8.33×10^{-13} °C
Rec. 2	3.13×10^{-11} °C	4.30×10^{-13} °C	1.81×10^{-13} °C
Rec. 3	3.05×10^{-11} °C	4.24×10^{-13} °C	1.70×10^{-13} °C

5.2. Layer bounded by two semi-infinite media

For the case of the layer placed between two semi-infinite media, the solution also needs to account for the continuity of temperature and heat fluxes at interface 1, since heat propagation also occurs through the top semi-infinite space (medium 0), which can be expressed by

$$\hat{T}_{02}(\omega,x,y,z)=\frac{-\mathrm{i}\pi}{L_y k_0}\sum_{n=1}^{N}A_{n0}^{b}\frac{k_n}{\nu_{n0}}J_0(k_n r)\mathrm{e}^{-\mathrm{i}\nu_{n0}|y|}, \tag{28}$$

where $\nu_{n0}=\sqrt{-(\mathrm{i}\omega/K_0)-k_n^2}$ with $\mathrm{Im}(\nu_{n0})\leq 0$.

The surface terms produced in interfaces 1 and 2 in media 1 and 2 (bottom semi-infinite medium) are expressed in Eqs. (21)–(23).

The coefficients A_{n0}^{b}, A_{n1}^{t}, A_{n1}^{b} and A_{n2}^{t} are defined by respecting the continuity of heat fluxes and temperatures at $y=h_1$ and 0. These surface conditions lead to the following system of four equations when the heat source is placed within the layer

$$\begin{bmatrix} -1 & -1 & \mathrm{e}^{-\mathrm{i}\nu_{n1}h_1} & 0 \\ -\dfrac{k_1\nu_{n1}}{k_0\nu_{n0}} & 1 & \mathrm{e}^{-\mathrm{i}\nu_{n1}h_1} & 0 \\ 0 & -\mathrm{e}^{-\mathrm{i}\nu_{n1}h_1} & 1 & 1 \\ 0 & \mathrm{e}^{-\mathrm{i}\nu_{n1}h_1} & 1 & -\dfrac{k_1\nu_{n1}}{k_2\nu_{n2}} \end{bmatrix}\begin{bmatrix} A_{n0}^{b} \\ A_{n1}^{t} \\ A_{n1}^{b} \\ A_{n2}^{t} \end{bmatrix}=\begin{bmatrix} b_1 \\ b_2 \\ b_3 \\ b_4 \end{bmatrix}, \tag{29}$$

where

$b_1=-\mathrm{e}^{-\mathrm{i}\nu_{n1}y_0}$,
$b_2=-\mathrm{e}^{-\mathrm{i}\nu_{n1}y_0}$,
$b_3=\mathrm{e}^{-\mathrm{i}\nu_{n1}|h_1-y_0|}$,
$b_4=-\mathrm{e}^{-\mathrm{i}\nu_{n1}|h_1-y_0|}$, when the source is in the layer $(0<y_0<h_1)$,

while

$b_1=\mathrm{e}^{-\mathrm{i}\nu_{n0}|y_0|}$,
$b_2=-(k_1\nu_{n1}/k_0\nu_{n0})\mathrm{e}^{-\mathrm{i}\nu_{n0}|y_0|}$,
$b_3=0$,
$b_4=0$, when the source is in the half-space $(y_0<h_1)$,

and

$b_1=0$,
$b_2=0$,
$b_3=\mathrm{e}^{-\mathrm{i}\nu_{n2}|h_1-y_0|}$,
$b_4=(k_1\nu_{n1}/k_2\nu_{n2})\mathrm{e}^{-\mathrm{i}\nu_{n2}|h_1-y_0|}$, when the source is in the half-space $(y_0>h_1)$.

The temperatures for the three media are then computed by adding the contribution of the source terms to those associated with the surface terms originated at the various interfaces. This procedure produces the following expressions for the temperatures in the three media

$$\begin{aligned}
\hat{T}(\omega,x,y,z)&=\frac{-\mathrm{i}\pi}{L_y k_0}\sum_{n=1}^{N}A_{n0}^{b}\frac{k_n}{\nu_{n0}}J_0(k_n r)\mathrm{e}^{-\mathrm{i}\nu_{n0}|y|}, \quad \text{if } y<0;\\
\hat{T}(\omega,x,y,z)&=\frac{\mathrm{e}^{-\mathrm{i}\sqrt{-(\mathrm{i}\omega/K_1)}r_0}}{2k_1 r_0}+\frac{-\mathrm{i}\pi}{L_y k_1}\sum_{n=1}^{N}J_0(k_n r)\frac{k_n}{\nu_{n1}}\\
&\quad\times(A_{n1}^{t}\,\mathrm{e}^{-\mathrm{i}\nu_{n1}|y|}+A_{n1}^{b}\,\mathrm{e}^{-\mathrm{i}\nu_{n1}|y-h|}), \quad \text{if } 0<y<h_1;\\
\hat{T}(\omega,x,y,z)&=\frac{-\mathrm{i}\pi}{L_y k_2}\sum_{n=1}^{N}A_{n2}^{t}\frac{k_n}{\nu_{n2}}J_0(k_n r)\mathrm{e}^{-\mathrm{i}\nu_{n2}|y-h_1|}, \quad \text{if } y>h_1.
\end{aligned} \tag{30}$$

The derivation presented assumed that the heat source is placed within the layer. However, the equations can be easily manipulated to accommodate another position of the source.

5.3. Multi-layer

The Green's functions for a multi-layer are established using the required boundary conditions at all interfaces.

Consider a system built from a set of m plane layers of infinite extent bounded by two flat, semi-infinite media, as shown in Fig. 6. The top semi-infinite medium is called medium 0, while the bottom semi-infinite medium is assumed to be the medium $m+1$. The thermal material properties and thickness of the various layers may differ. The system of equations is achieved considering that the multi-layer is excited by a heat source located in the first layer (medium 1). The heat field is computed at some position in the domain, taking into account both the surface heat terms generated at each interface and the contribution of the heat source term.

For the layer j, the heat surface terms on the upper and lower interfaces can be expressed as

$$\begin{aligned}
\hat{T}_{j1}(\omega,x,y,z)&=\frac{-\mathrm{i}\pi}{L_y k_j}\sum_{n=1}^{N}A_{nj}^{t}\frac{k_n}{\nu_{nj}}J_0(k_n r)\mathrm{e}^{-\mathrm{i}\nu_{nj}|y-\sum_{l=1}^{j-1}h_l|},\\
\hat{T}_{j2}(\omega,x,y,z)&=\frac{-\mathrm{i}\pi}{L_y k_j}\sum_{n=1}^{N}A_{nj}^{b}\frac{k_n}{\nu_{nj}}J_0(k_n r)\mathrm{e}^{-\mathrm{i}\nu_{nj}|y-\sum_{l=1}^{j}h_l|},
\end{aligned} \tag{31}$$

where $\nu_{nj}=\sqrt{(-\mathrm{i}\omega/K_j)-k_n^2}$, with $\mathrm{Im}(\nu_{nj})\leq 0$ and h_1 is the thickness of the layer l. The heat surface terms produced at interfaces 1 and $m+1$, which govern the heat that propagates through the top and bottom semi-infinite media, are, respectively, expressed by

$$\begin{aligned}
\hat{T}_{02}(\omega,x,y,z)&=\frac{-\mathrm{i}\pi}{L_y k_0}\sum_{n=1}^{N}A_{n0}^{b}\frac{k_n}{\nu_{n0}}J_0(k_n r)\mathrm{e}^{-\mathrm{i}\nu_{n0}|y|}, \quad \text{and}\\
\hat{T}_{(m+1)2}(\omega,x,y,z)&=\frac{-\mathrm{i}\pi}{L_y k_{(m+1)}}\\
&\quad\times\sum_{n=1}^{N}A_{n(m+1)}^{t}\frac{k_n}{\nu_{n(m+1)}}J_0(k_n r)\mathrm{e}^{-\mathrm{i}\nu_{n(m+1)}|y-\sum_{l=1}^{m}h_l|}.
\end{aligned} \tag{32}$$

A system of $2(m+1)$ equations is derived, ensuring the continuity of temperatures and heat fluxes along the $m+1$

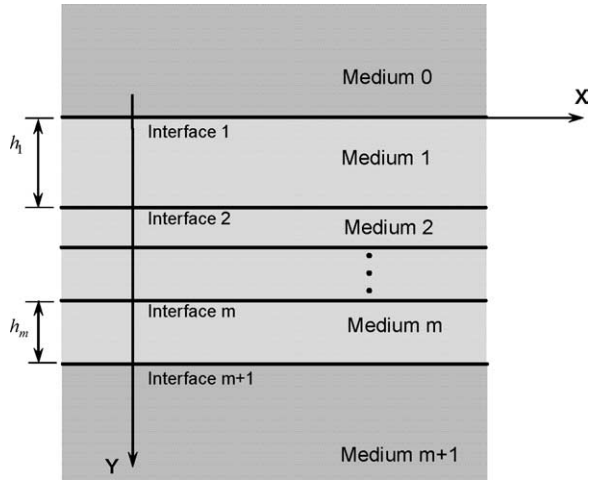

Fig. 6. Geometry of the problem for a multi-layer bounded by two semi-infinite media.

interfaces between layers. Each equation takes into account the contribution of the surface terms and the involvement of the incident field. All the terms are organized according to the form $\underline{\underline{F}}\,\underline{a} = \underline{b}$

$$\begin{bmatrix}
1 & 1 & -e^{-i\nu_{n1}h_1} & \cdots & 0 & 0 & 0 \\
\frac{1}{k_0\nu_{n0}} & -\frac{1}{k_1\nu_{n1}} & -\frac{e^{-i\nu_{n1}h_1}}{k_1\nu_{n1}} & \cdots & 0 & 0 & 0 \\
0 & -e^{-i\nu_{n1}h_1} & 1 & \cdots & 0 & 0 & 0 \\
0 & \frac{e^{-i\nu_{n1}h_1}}{k_1\nu_{n1}} & \frac{1}{k_1\nu_{n1}} & \cdots & 0 & 0 & 0 \\
\cdots & \cdots & \cdots & \cdots & \cdots & \cdots & \cdots \\
0 & 0 & 0 & \cdots & 1 & -e^{-i\nu_{nm}h_m} & 0 \\
0 & 0 & 0 & \cdots & -\frac{1}{k_m\nu_{nm}} & -\frac{e^{-i\nu_{nm}h_m}}{k_m\nu_{nm}} & 0 \\
0 & 0 & 0 & \cdots & -e^{-i\nu_{nm}h_m} & 1 & 1 \\
0 & 0 & 0 & \cdots & \frac{e^{-i\nu_{nm}h_m}}{k_m\nu_{nm}} & \frac{1}{k_m\nu_{nm}} & -\frac{1}{k_{(m+1)}\nu_{n(m+1)}}
\end{bmatrix}$$

$$\begin{bmatrix} A^b_{n0} \\ A^t_{n1} \\ A^b_{n1} \\ \cdots \\ A^t_{nm} \\ A^b_{nm} \\ A^t_{n(m+1)} \end{bmatrix} = \begin{bmatrix} e^{-i\nu_{n1}y_0} \\ \frac{1}{k_1\nu_{n1}}e^{-i\nu_{n1}y_0} \\ e^{-i\nu_{n1}|h_1-y_0|} \\ -\frac{1}{k_1\nu_{n1}}e^{-i\nu_{n1}|h_1-y_0|} \\ \cdots \\ 0 \\ 0 \\ 0 \\ 0 \end{bmatrix}. \tag{33}$$

The resolution of the system gives the amplitude of the surface terms in each interface. The temperature field for each layer formation is obtained by adding these surface terms to the contribution of the incident field, leading to the following equations.

Top semi-infinite medium (*medium 0*)

$$\hat{T}(\omega,x,y,z) = \frac{-i\pi}{L_y k_0}\sum_{n=1}^{N} A^b_{n0}\frac{k_n}{\nu_{n0}}J_0(k_n r)e^{-i\nu_{n0}|y|}, \quad \text{if } y<0;$$

layer 1 (source position)

$$\hat{T}(\omega,x,y,z) = \frac{e^{-i\sqrt{-(i\omega/K_1)}r_0}}{2k_1 r_0} + \frac{-i\pi}{L_y k_1}\sum_{n=1}^{N} J_0(k_n r)\frac{k_n}{\nu_{n1}} \times (A^t_{n1}\,e^{-i\nu_{n1}|y|} + A^b_{n1}\,e^{-i\nu_{n1}|y-h_1|}), \quad \text{if } 0<y<h_1;$$

layer j ($j\neq 1$)

$$\hat{T}(\omega,x,y,z) = \frac{-i\pi}{L_y k_j}\sum_{n=1}^{N} J_0(k_n r) \times \frac{k_n}{\nu_{nj}}\left(A^t_{nj}\,e^{-i\nu_{nj}|y-\sum_{l=1}^{j-1}h_l|} + A^b_{nj}\,e^{-i\nu_{nj}|y-\sum_{l=1}^{j}h_l|}\right),$$

$$\text{if } \sum_{l=1}^{j-1}h_l < y < \sum_{l=1}^{j}h_l;$$

bottom semi-infinite medium (*medium m+1*)

$$\hat{T}(\omega,x,y,z) = \frac{-i\pi}{L_y k_{(m+1)}} \times \sum_{n=1}^{N} A^t_{n(m+1)}\frac{k_n}{\nu_{n(m+1)}}J_0(k_n r)e^{-i\nu_{n(m+1)}|y-\sum_{l=1}^{m}h_l|}. \tag{34}$$

Notice that when the position of the heat source is changed, the matrix $\underline{\underline{F}}$ remains the same, while the independent terms of $\underline{b}$ are different. However, as the equations can be easily manipulated to consider another position for the source, they are not included here.

5.4. Verification of the solution

Next, the results are found for the three scenarios. First, a flat layer, 2.0 m thick, is assumed to be bounded by one half-space. Null heat fluxes or null temperatures are prescribed at the top surface. Then, a flat layer, also 2.0 m thick, bounded by two semi-infinite media, is used to evaluate the accuracy of the proposed formulation. The thermal material properties used in the intermediate layer are $k=1.4\ \mathrm{W\,m^{-1}\,^{\circ}C^{-1}}$, $c=880.0\ \mathrm{J\,kg^{-1}\,^{\circ}C^{-1}}$ and $\rho=2300.0\ \mathrm{kg\,m^{-3}}$, while at the top and bottom media they are $k=63.9\ \mathrm{W\,m^{-1}\,^{\circ}C^{-1}}$, $c=434.0\ \mathrm{J\,kg^{-1}\,^{\circ}C^{-1}}$ and $\rho=7832.0\ \mathrm{kg\,m^{-3}}$.

The calculations have been performed in the frequency domain from 0.0 to 320.0×10^{-7} Hz. The amplitude of the response for four receivers placed in two different media was computed for a heat point source applied at (0.0,1.0,0.0) m. The real and imaginary parts of the full response at receivers

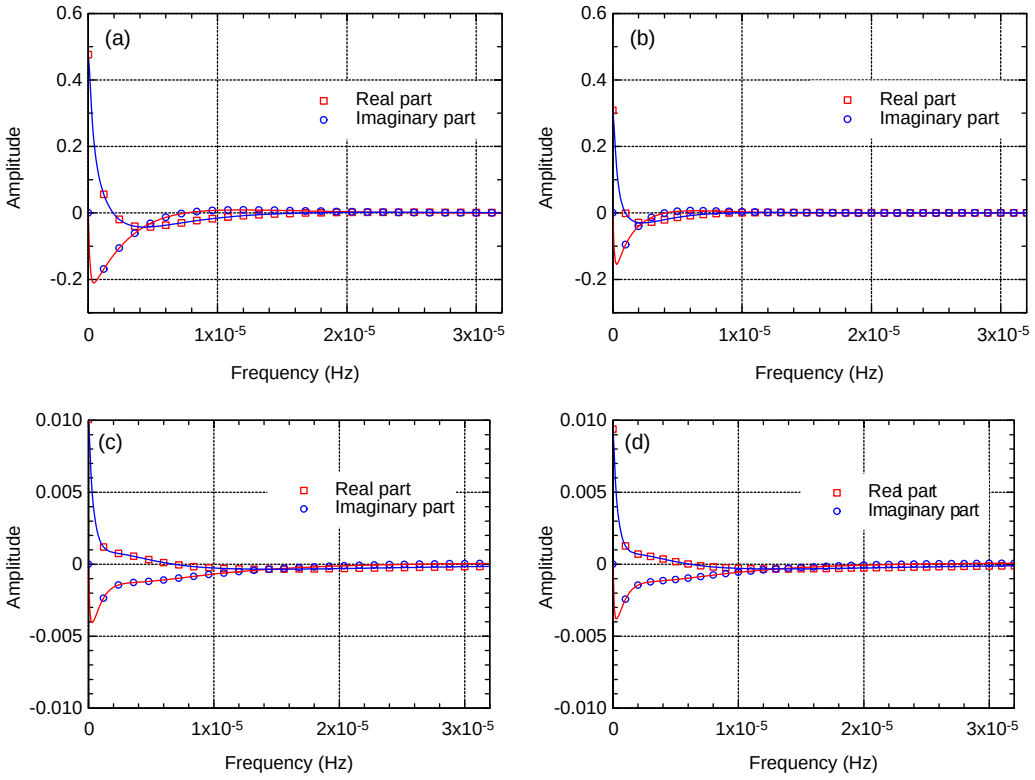

Fig. 7. Null heat flux at $y=0$ (*Case I*): real and imaginary parts of the responses for a layer over a half-space at different receivers: (a) Rec. 1; (b) Rec. 2; (c) Rec. 4; (d) Rec. 5.

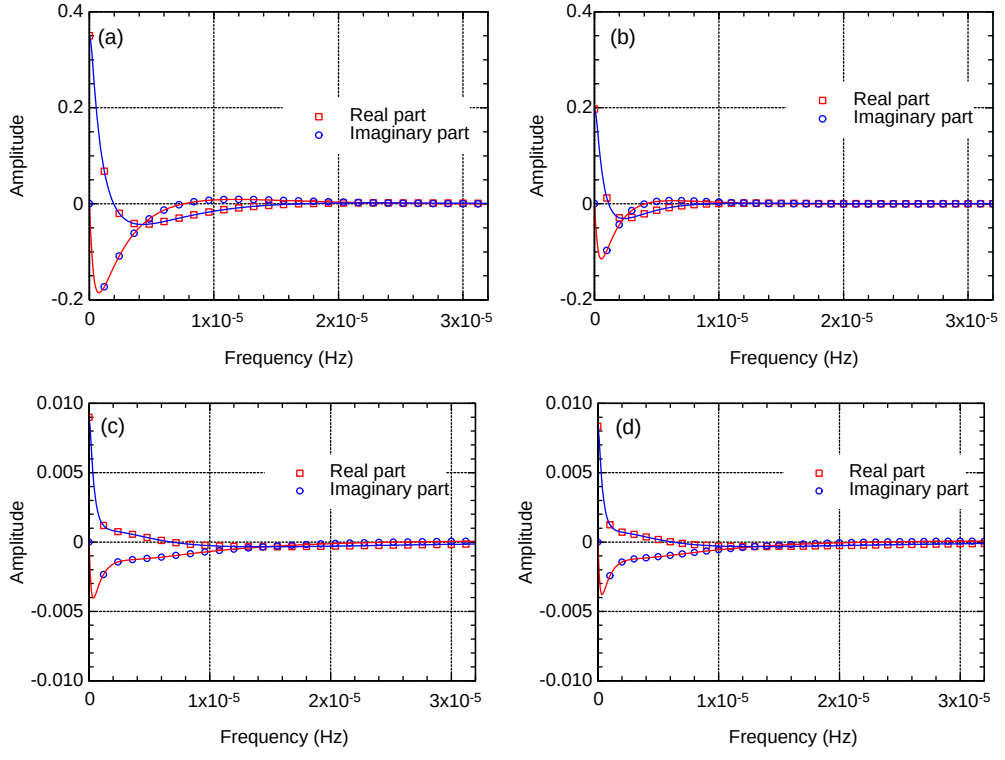

Fig. 8. Null temperature at $y=0$ (*Case II*): real and imaginary parts of the responses for a layer over a half-space at different receivers: (a) Rec. 1; (b) Rec. 2; (c) Rec. 4; (d) Rec. 5.

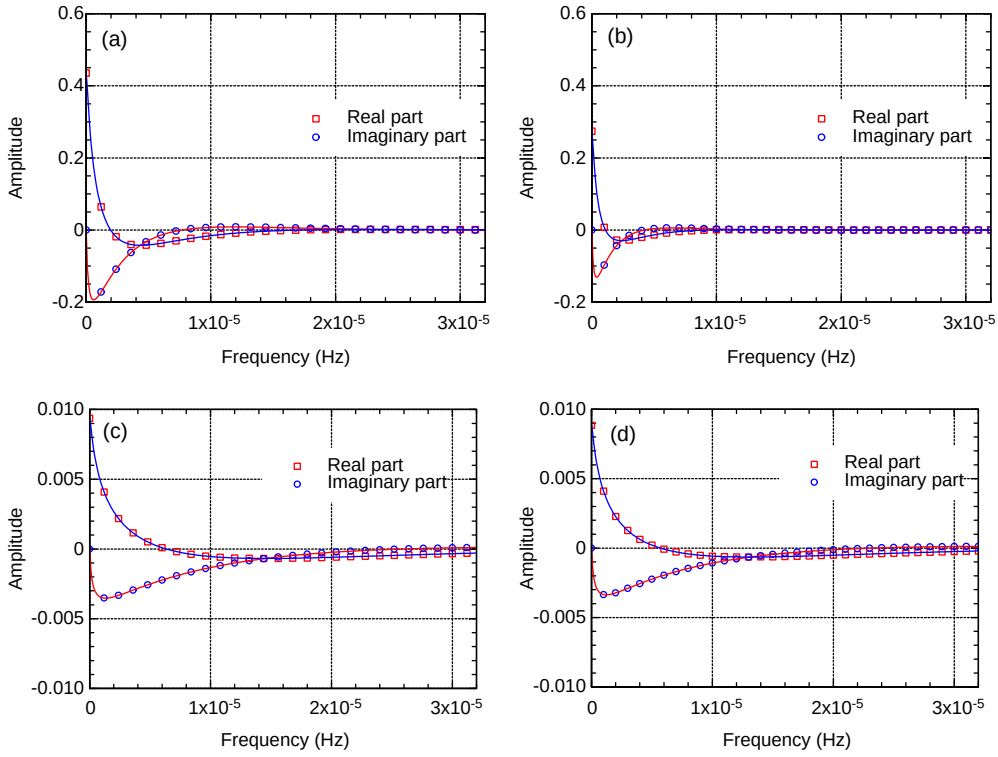

Fig. 9. Real and imaginary parts of the responses for a layer bounded by two semi-infinite media at different receivers: (a) Rec. 1; (b) Rec. 2; (c) Rec. 4; (d) Rec. 5.

Rec. 1 (0.2,0.5,0.0) m, Rec. 2(0.2,0.5,0.5) m, Rec. 4 (0.2,2.5,0.0) m and Rec. 5 (0.2,2.5,0.5) m are displayed in Figs. 7–9. The solid lines represent the analytical responses computed using the proposed Green's functions, while the marked points correspond to the 2.5D formulation [3] solution.

As can be seen, these two solutions seem to be in very close agreement, and equally good results were obtained from tests in which heat sources and receivers were situated at different points.

6. Conclusions

Three-dimensional Green's functions for computing the transient heat transfer by conduction in an unbounded medium, half-space, slab and layered media have been presented. The transient heat responses generated by a spherical heat source were first obtained in the frequency domain. Time solutions were then obtained after the application of an inverse Fourier transform in the frequency domain.

The proposed analytical solutions were obtained after writing the response of a spherical heat source as a sum of Bessel integrals, assuming a set of sources equally spaced along the vertical direction. The results for a layered formation are obtained by adding the heat source term and the surface terms required to satisfy the interface boundary conditions (temperature and heat flux continuity).

The unbounded medium formulation was verified by comparing its time responses with the exact known time solution. In turn, the proposed analytical solutions used in the half-space, slab systems and layered media formulation were compared against the frequency responses obtained when a double space Fourier transformation was applied along the horizontal directions [3]. Therefore, the present formulation involves less computational effort than the previous solution. In addition, time responses provided by the proposed formulation were compared with those provided by analytical solutions, known for simpler cases such as the half-space and the slab formations.

The proposed Green's functions can be used as fundamental solutions in BEM or MFS algorithms for solving layered formations containing buried three-dimensional inclusions, while the analytical solutions obtained before [3] are better suited to resolving the case of layered formulations containing cylindrical inclusions.

References

[1] Sommerfeld A. Mechanics of deformable bodies. New York: Academic Press; 1950.
[2] Ewing WM, Jardetzky WS, Press F. Elastic waves in layered media. New York: McGraw-Hill; 1957.
[3] Tadeu A, António J, Simões N. 2.5D Green's functions in the frequency domain for heat conduction problems in unbounded, half-space, slab and layered media. CMES: Comput Model Eng Sci 2004;6(1):43–58.
[4] Carslaw HS, Jaeger JC. Conduction of heat in solids. 2nd ed. New York: Oxford University Press; 1959.
[5] Bouchon M, Aki K. Discrete wave-number representation of seismic-source wave field. Bull Seismol Soc Am 1977;67:259–77.
[6] Kausel E, Roesset JM. Frequency domain analysis of undamped systems. J Eng Mech ASCE 1992;118(4):721–34.
[7] Banerjee PK. The boundary element methods in engineering. England: McGraw-Hill; 1981.